A framework for correcting measurement position and directions to improve experimental frequency-based substructuring and hybrid models

M. Brons [1,2], **F. Trainotti** [2]
[1] Technical University of Denmark, Department of Civil and Mechanical Engineering,
Nils Koppels Allé, 2800, Kgs. Lyngby, Denmark

[2] Technical University of Munich, Department of Mechanical Engineering,
Chair of Applied Mechanics, Munich Institute for Robotics and Machine Intelligence,
Boltzmannstraße 15, 85748 Garching bei München
e-mail: **maribr@dtu.dk**

Abstract

Experimental Frequency-based substructuring (FBS) is a strong tool for coupling individual substructures in the frequency domain to obtain predictions of the coupled response. A high-fidelity hybrid model can be obtained using FBS experimental measurements combined with an underlying numerical model. However, if the experimental sensor and impact positions are not exactly as numerically defined, the hybrid model will propagate errors. In this work, we suggest a method for correcting the position and direction of an impact/sensor to obtain more robust hybrid models. The framework is initially implemented on numerical data to investigate how direction or position can be detected. It is also tested on experimental data of a beam to validate the framework's applicability in practice.

1 Introduction

Experimental Frequency-based substructuring is a valuable tool for obtaining predictions of complex coupled structures [1]. The quality of an obtained coupled response relies on multiple factors [2]. The measurement error emitting from equipment limits is one unavoidable issue. However, an avoidable issue is the inaccurately defined positioning and direction of sensors and impacts. When designing a substructuring measurement campaign, multiple impacts are planned at different positions and directions on the structure. Here, it is customary to assume the impacts to be purely in one principal direction, even though such a perfect hit is unfeasible to obtain manually. Likewise, the defined positions are also approximate, as a hammer tip has a certain width, and the individual performing the experiments might also hit the structure slightly inaccurately. Repeating hits at each position three times or more is good practice. With such repetitions, the coherence between the repetitions can reveal inconsistencies in the average, but the coherence cannot reveal a bias, such as a positioning error.

A slight shift in an impact position will influence the position of the antiresonances. Mostly, dynamicists do not care much about antiresonances, as there is little energy in the response at these frequencies. However, when coupling, the wrong position of an antiresonance can propagate in an unfortunate way. Likewise, a slight shift in the direction of an impact influences the resonant peaks present in a response. If the impact direction differs from the plan, additional modes may be excited. Both issues will influence the coupled response negatively.

Figure 1 demonstrates the challenge of impact uncertainty. When impacting a structure with a hammer, there is a limit to the accuracy of the impact position. The impact will be within some area of likelihood. The size of the area depends on the type of hammer, its tip width, and who performs the experiment. Considering

a standard impact hammer, an area with a radius of 2 mm is not unlikely. Sometimes, we also make plain mistakes and impact the wrong position, and then even 10-20 mm shifts can occur. In this work, we consider plain mistakes to be a separate category from measurement uncertainties. At first glance, a shift of 2 mm can appear insignificant; however, in some cases, it is not. Consider a slender beam; the response is quite different if hit right at a nodal point of a bending mode compared to slightly next to the nodal point.

Several works demonstrates the challenge with FBS coupling in practice, due to noise and uncertainties [3, 4], and decoupling using FBS is even more sensitive to such problems [5]. Recent work [6] suggests a method to identify and remove such biased data to have better data to use for experimental substructuring. The method is based on the method of System Equivalent Model Mixing (SEMM) [7]. In this work, we suggest a method that uses similar principles to correct the position and direction of an impact (instead of removing the data) to obtain robust hybrid models. With this correction, the experiment can also be performed with less attention to detail, as deviations from the plan are correctable afterwards. In the following section, we will present the basics of the SEMM method and show how it is used in the framework for correcting measurement positions.

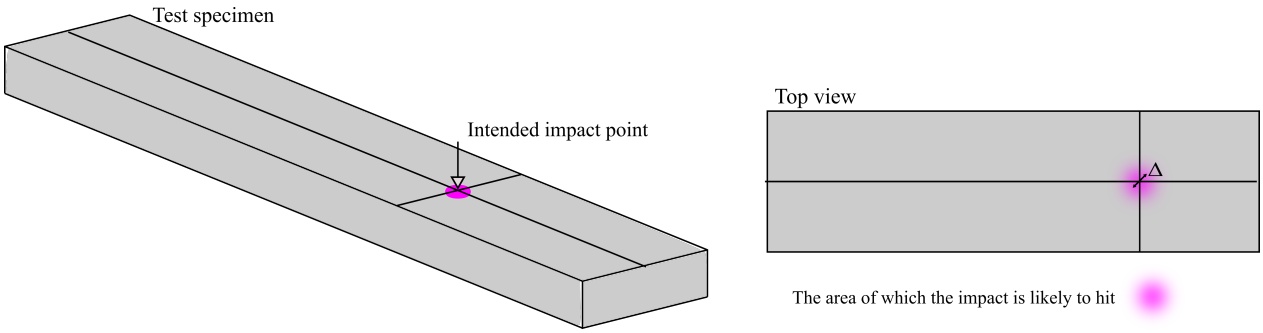

Figure 1: Demonstration of the problem.

2 System Equivalent Model Mixing (SEMM)

System Equivalent Model Mixing (SEMM) is a Frequency-Based Substructuring (FBS) approach for updating models [7]. The method is useful when a high-fidelity numerical model is available, but the model's predictions do not entirely agree with experimental vibration measurements. In contrast to a FEM model, available experimental data is usually sparse. Vibration data is often only available from a few accelerometers, measuring the response after a handful of impacts. The experimental data only sometimes suffices on its own. SEMM allows the combination of experimental data with a high-fidelity model. The effect is a hybrid model with high fidelity that is 'tuned' to the experimental data.

We set up the SEMM equations by first introducing Frequency-based Substructuring (FBS), using the Lagrange-Multiplier (LM) approach [1]:

$$\begin{cases} \boldsymbol{u} = \mathbf{Y}^{\mathrm{A|B}}(\boldsymbol{f} - \mathbf{B}^{\mathrm{T}}\boldsymbol{\lambda}) \\ \mathbf{B}\,\boldsymbol{u} = \mathbf{0} \end{cases}, \qquad \mathbf{Y}^{\mathrm{A|B}} = \begin{bmatrix} \mathbf{Y}^{\mathrm{A}} & \mathbf{0} \\ \mathbf{0} & \mathbf{Y}^{\mathrm{B}} \end{bmatrix}, \tag{1}$$

where $\mathbf{Y}^{\mathrm{A|B}}$ is a block matrix containing the responses of substructure A and B, measured separately. Substructure A and B are then coupled via the interface forces $\mathbf{g} = \mathbf{B}^{\mathrm{T}}\boldsymbol{\lambda}$, with $\boldsymbol{\lambda}$ being the interface force intensities, and $\mathbf{B}$ a Boolean matrix matching the connection DoFs. By rearranging the above equations, we obtain the standard coupling equation [1]:

$$\hat{\mathbf{Y}}^{\mathrm{AB}} = \left[\mathbf{I} - \mathbf{Y}^{\mathrm{A|B}}\mathbf{B}^{\mathrm{T}}\left(\mathbf{B}\mathbf{Y}^{\mathrm{A|B}}\mathbf{B}^{\mathrm{T}}\right)^{-1}\mathbf{B}\right]\mathbf{Y}^{\mathrm{A|B}}. \tag{2}$$

Note, the single-line coupling results in redundant DoFs, as the DoFs of connection will appear twice, since $\hat{\mathbf{Y}}^{\mathrm{AB}}$ is the same size as $\mathbf{Y}^{\mathrm{A|B}}$. The SEMM method follows the same principle, here we however have three datasets in the block matrix, as we decouple and couple in one step:

$$\begin{cases} \boldsymbol{u} = \mathbf{Y}^{\mathrm{block}}(\boldsymbol{f} - \mathbf{B}^{\mathrm{T}}\boldsymbol{\lambda}) \\ \mathbf{B}\,\boldsymbol{u} = \mathbf{0} \end{cases}, \qquad \mathbf{Y}^{\mathrm{block}} = \begin{bmatrix} \mathbf{Y}^{\mathrm{all}}_{par} & \mathbf{0} & \mathbf{0} \\ \mathbf{0} & -\mathbf{Y}^{\mathrm{rem}}_{par} & \mathbf{0} \\ \mathbf{0} & \mathbf{0} & \mathbf{Y}^{\mathrm{exp}} \end{bmatrix}, \tag{3}$$

where the block matrix contains the large parent model $\mathbf{Y}^{\mathrm{all}}_{par}$, the response at the DoFs to be removed $\mathbf{Y}^{\mathrm{rem}}_{par}$, and the experimental response $\mathbf{Y}^{\mathrm{exp}}$ (often called the overlay model). Now $\mathbf{B}$ is the Boolean matrix matching the corresponding removed parent DoFs as well as removed overlay DoFs. As, with the standard FBS, we can rearrange the equations above, and the hybrid model is given by

$$\hat{\mathbf{Y}}^{\mathrm{hybrid}}_{\mathrm{all}} = \left[\mathbf{I} - \mathbf{Y}^{\mathrm{block}}\mathbf{B}^{\mathrm{T}}\left(\mathbf{B}\mathbf{Y}^{\mathrm{block}}\mathbf{B}^{\mathrm{T}}\right)^{-1}\mathbf{B}\right]\mathbf{Y}^{\mathrm{block}}, \tag{4}$$

where $\hat{\mathbf{Y}}^{\mathrm{hybrid}}_{\mathrm{all}}$ is the same size as the block matrix, and contains redundant DoFs. Figure 2 demonstrates the SEMM principle. Note, the responses at DoFs that are not experimentally measured (steel blue in the figure) change with the SEMM process, as the force equilibrium and compatibility conditions has to be fulfilled. Retaining only the primary DoFs (thus getting rid of the redundant DoFs), the SEMM equation can be rewritten to [7]:

$$\hat{\mathbf{Y}}^{\mathrm{hybrid}} = \mathbf{Y}^{\mathrm{all}}_{par} - \begin{bmatrix} \mathbf{Y}_{ir} \\ \mathbf{Y}_{rr} \end{bmatrix}_{par} \left(\mathbf{Y}^{\mathrm{rem}}_{rr,par}\right)^{-1}\left(\mathbf{Y}^{\mathrm{rem}}_{rr,par} - \mathbf{Y}^{\mathrm{exp}}\right)\left(\mathbf{Y}^{\mathrm{rem}}_{rr,par}\right)^{-1}\begin{bmatrix} \mathbf{Y}_{ri} & \mathbf{Y}_{rr} \end{bmatrix}_{par}, \tag{5}$$

where the is are the internal DoFs of the parent numerical model, and the rs are the DoFs to be removed. Note that $\mathbf{Y}^{\mathrm{rem}}_{rr,par}$ is here the same matrix as $\mathbf{Y}^{\mathrm{rem}}_{par}$ used in (3), but for notation consistency we have added the subscript rr.

For robustness, it is however recommended to use the *extended* SEMM [7], which extends the compatibility and equilibrium of the parent-removed connection to include internal DoFs. The final extended SEMM method can thus be written in a single line as:

$$\mathbf{Y}^{\mathrm{hybrid}} = \mathbf{Y}^{\mathrm{all}}_{par} - \mathbf{Y}^{\mathrm{all}}_{par}\left(\begin{bmatrix} \mathbf{Y}_{ri} & \mathbf{Y}_{rr} \end{bmatrix}^{\mathrm{rem}}_{par}\right)^{+}\left(\mathbf{Y}^{\mathrm{rem}}_{rr,par} - \mathbf{Y}^{\mathrm{exp}}\right)\left(\begin{bmatrix} \mathbf{Y}_{ir} \\ \mathbf{Y}_{rr} \end{bmatrix}^{\mathrm{rem}}_{par}\right)^{+}\mathbf{Y}^{\mathrm{all}}_{par}, \tag{6}$$

where $^{+}$ is the pseudo inverse. For more details on the extended method cf. [7]. The equation demonstrates that by having a numerical model with DoFs coinciding with the experimental DoFs, a hybrid model can be obtained, by only a single line.

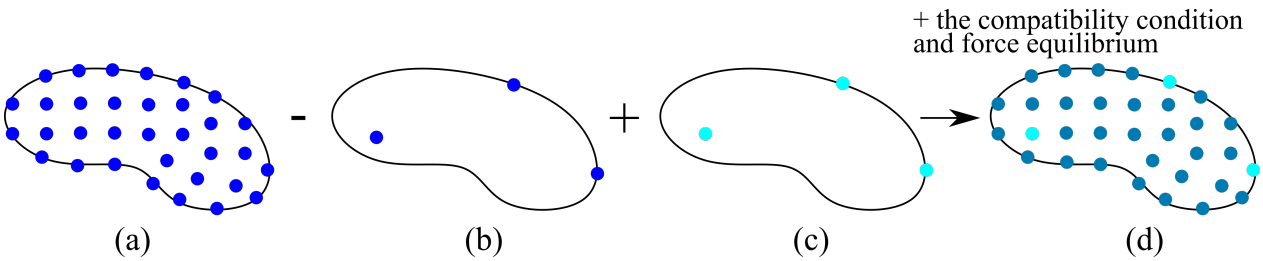

Figure 2: SEMM method; a) high fidelity parent model (blue), b) removing selected DoFs of the parent model, (c) adding experimental measurement points (cyan), also called the overlay model. Enforcing force equlibrium and compatability between the overlay and the trimmed parent model, all the non-measured dofs of the hybrid model (d) will be tuned to the experiment (steel blue).

3 Framework for correcting measurement data

In [6], a method to identify inconsistent measurements is proposed. In this work, we apply the same method. However, we extend it, so when we identify an inconsistency, we try to correct the measurement's associated *meta data* by slightly updating the predefined position and direction of the recorded data point. For clarification, the measurement data is not changed or filtered; but we compare the measured responses to various closely defined DoFs of the numerical model. Figure 3 visualizes the framework. It requires two iterations. The inner process (+ Step 4) is identical to that of [6]. The novelty is the outer process, where we update the positions and repeat the correlation check. Note, Step 2 applies the extended SEMM model (6).

In most cases, we can improve correlations significantly by shifting the defined positions a tiny bit, thus avoiding discarding the experimental data point. In some cases, a measurement is actually of poor quality (this can be due to many things, e.g. double hits). In that case, we discard the measurement. The threshold for discarding measurements depends on the specific setup [6]. If the noise level and damping of the specimen are generally high, it may not be possible to get perfect correlations. However, in the free-free beam test case we will investigate, we can require a very high correlation, as the damping is low, and the general S/N ratio is good.

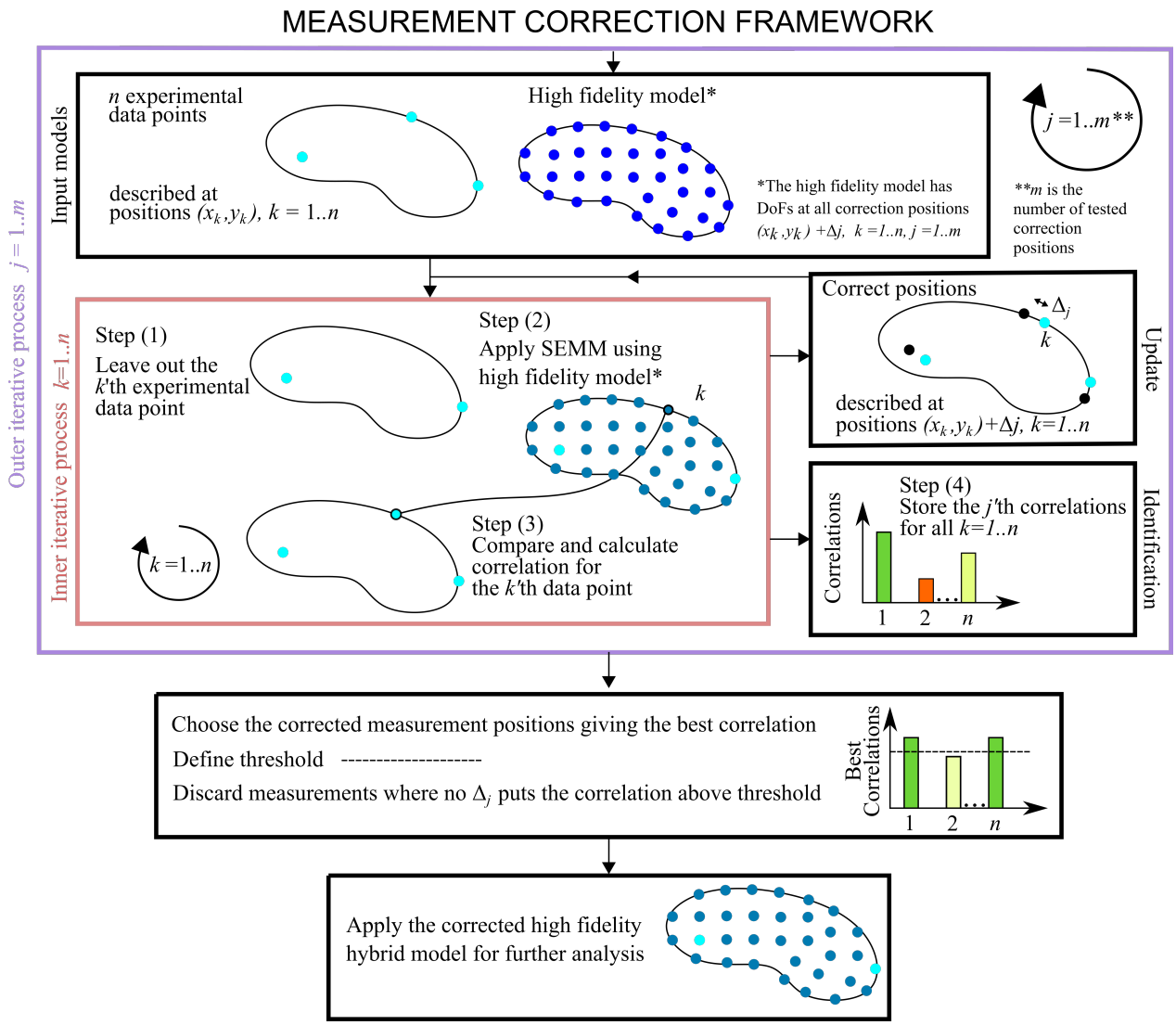

Figure 3: Proposed algorithm for identifying inconsistent measurements and correcting their positions. The iterative processes will be the same regardless the type of correction (impacts/sensors, position/direction).

3.1 Coherence as Criterion

The framework require a measure for correlation. In principle it could be anything, such as the Local Assurance Criteria or Frequency Response Assurance Criteria [6]. It can be the mean or the standard deviation, or the coherence in a limited frequency area. We use the average coherence over the frequency-span as criterion for the accuracy of the meta data (position and direction), as in [6]. The coherence is calculated as:

$$\mathrm{COH}_{ij}(\omega_n) = \frac{\left(\mathrm{Y}_{ij}^{\mathrm{Recon}}(\omega_n) + \mathrm{Y}_{ij}^{\mathrm{exp}}(\omega_n)\right)\left(\mathrm{Y}_{ij}^{\mathrm{Recon}^*}(\omega_n) + \mathrm{Y}_{,ij}^{\mathrm{exp}^*}(\omega_n)\right)}{2\left(\mathrm{Y}_{ij}^{\mathrm{Recon}^*}(\omega_n)\mathrm{Y}_{ij}^{\mathrm{Recon}}(\omega_n) + \mathrm{Y}_{ij}^{\mathrm{exp}*}(\omega_n)\mathrm{Y}_{,ij}^{\mathrm{exp}}(\omega_n)\right)}, \tag{7}$$

where $\mathrm{Y}_{ij}^{\mathrm{exp}}$ is real measurement after impact i at sensor j, and $\mathrm{Y}_{ij}^{\mathrm{Recon}}$ is its reconstructed counterpart (the steel-blue result of Step 2), and $*$ denotes the complex conjugate. The mean over the measured frequency range is then

$$\overline{\mathrm{COH}}_{ij} = \frac{1}{N}\sum_{n=1}^{N}\mathrm{COH}_{ij}(\omega_n), \tag{8}$$

where N is the number of frequency lines in a response. Other options are to consider the minimum coherence over the range.

Table 1: Parent model natural frequencies and modes shapes. *The experimentally measured natural frequencies are not used in numerical validation section, but in the following experimental section, Section 5.

Mode	ω_n^{par} [Hz]	ω_n^{exp} [Hz]*	Type of mode	Visualization
1	268.5	268.6	1st z-bending	
2	739.4	738.1	2nd z-bending	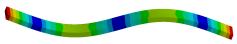
3	1239.0	1241.3	1st y-torsion	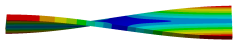
4	1447.4	1444.4	3rd z-bending	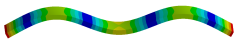
5	1492.1	1489.2	1st x-bending	
6	2386.6	2378.4	4th z-bending	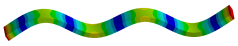
7	2501.4	2507.5	2nd y-torsion	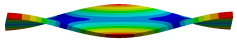
8	3551.6	3536.9	5th z-bending	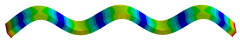
9	3794.8	3786.3	2nd x-bending	
10	3809.5	3819.2	3rd y-torsion	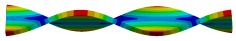

4 Numerical validation

To validate the framework presented in Figure 3, we test it on a simple numerical beam with free-free boundary conditions. The beam is of the dimensions $49.6 \times 400 \times 8.5$ mm^3, see Figure 4. The model will

also act as the parent model in the experimental test in Section 5. The beam has 10 numerically calculated natural frequencies between 0 - 4000 kHz, as shown in Table 1. The beam mesh is generated in ANSYS, then exported and the following analysis is performed in Python, using the Open-source software package PyFBS [8].

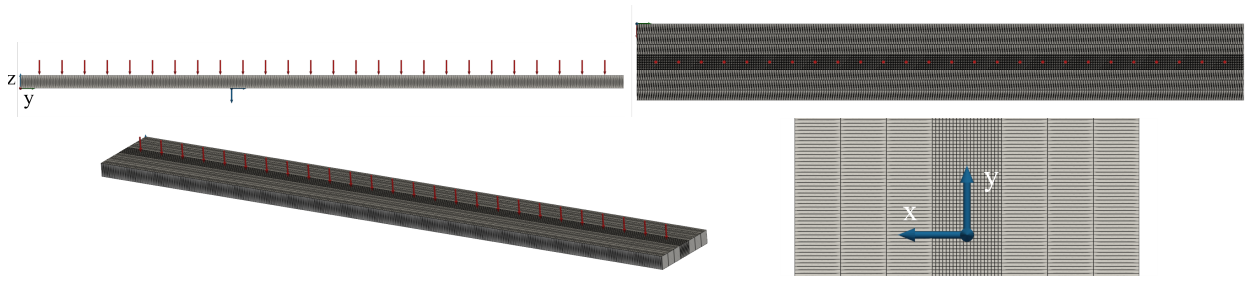

Figure 4: The numerical model is designed to have an extra high resolution around the impact and sensor positions so the small shifts are possible.

We validate the framework by taking a set of DoFs of the numerical model as experimental data points. The data points we pollute with noise and purposely define their position as neighbors to their actual positions. The parent model data is based on one triaxial accelerometer under the beam at the center, in the longitudinal position 140 mm, Figure 4. The beam's top side is subject to 26 impacts along the length. The impacts start at 12.5 mm and are evenly distributed with a spacing of 15 mm. The simulated experimental data are almost at the same positions but with random shifts between 0-2 mm in the x and y directions. To apply the SEMM method, the numerical model must have coinciding DoFs with the experimental DoFs. Therefore, the numerical model has a fine resolution of 0.5 mm at $\pm$ 2.5 mm on both sides of the center line; see Figure 4. The numerical positions and the exact shifts (randomly chosen) enforced on the simulated experimental data are shown in Table 2. Figure 5 shows an example of one of the generated FRFs (Impact 25). The noise enforced on the simulated experimental data is Gaussian complex noise, scaled via four terms: $\eta_{1-4} = [2e^{-3}, 2e^{-4}, 2e^{-2}, 2e^{-4}]$. The first two are proportional to the real and imaginary part, respectively, and the last two are base-level noise on both the real and imaginary part [8]. The modal damping is set to 0.001. We identify the average coherence given the original positions by running the identification part of the framework (Steps 1-4 in Figure 3). Figure 6 shows the result. Noticeably, the originally defined positions result in relatively poor coherence for several impacts, especially Impact 25, although the position shift is only 2.0 mm. The poor coherence also demonstrates that performing this positional updating is not a waste of time; slight shifts make a difference in the predicted response.

Table 2: Original parent model impact positions and shifts used on the simulated experimental data in mm. The accelerometer shift is -1 mm in x-direction and 0.5 mm in y-direction.

Impact	1	2	3	4	5	6	7	8	9	10	11	12	13
Parent x-pos	24.8	24.8	24.8	24.8	24.8	24.8	24.8	24.8	24.8	24.8	24.8	24.8	24.8
Exp. x shift	-1.0	-1.0	0.5	-0.5	1.0	1.5	1.0	-1.0	-1.0	0.0	0.0	0.0	-0.5
Parent y-pos	12.5	27.5	42.5	57.5	72.5	87.5	102.5	117.5	132.5	147.5	162.5	177.5	192.5
Exp. y shift	1.0	0.0	1.5	-1.5	0.0	0.0	-1.0	0.5	0.5	-0.5	1.0	0.0	0.0
Impact	14	15	16	17	18	19	20	21	22	23	24	25	26
Parent x-pos	24.8	24.8	24.8	24.8	24.8	24.8	24.8	24.8	24.8	24.8	24.8	24.8	24.8
Exp. x shift	1.5	0.5	0.0	0.0	-1.5	1.0	1.0	0.0	0.0	-0.5	0.5	0.0	0.0
Parent y-pos	207.5	222.5	237.5	252.5	267.5	282.5	297.5	312.5	327.5	342.5	357.5	372.5	387.5
Exp. y shift	-1.0	0.0	-1.0	-2.0	1.0	2.0	-1.0	1.0	0.0	0.0	1.0	2.0	1.0

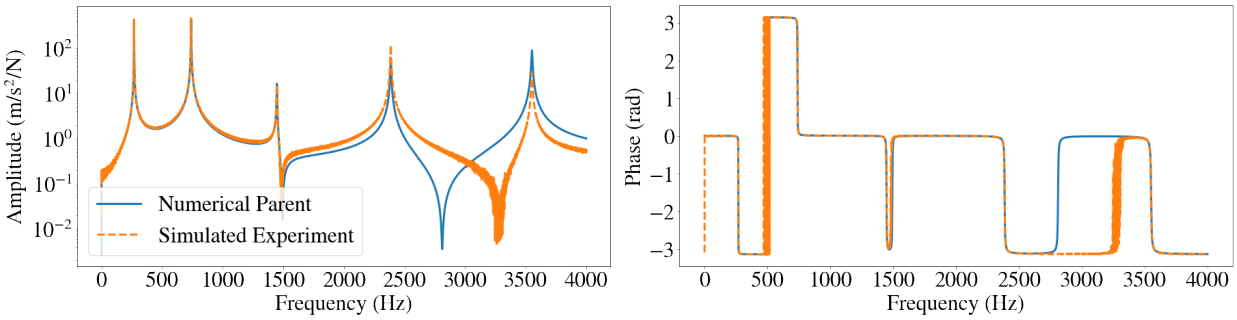

Figure 5: Example FRF of the parent model and the simulated measured response (noise + position shift). The z response of the accelerometer, after Impact 25 at the y position 372.5 mm.

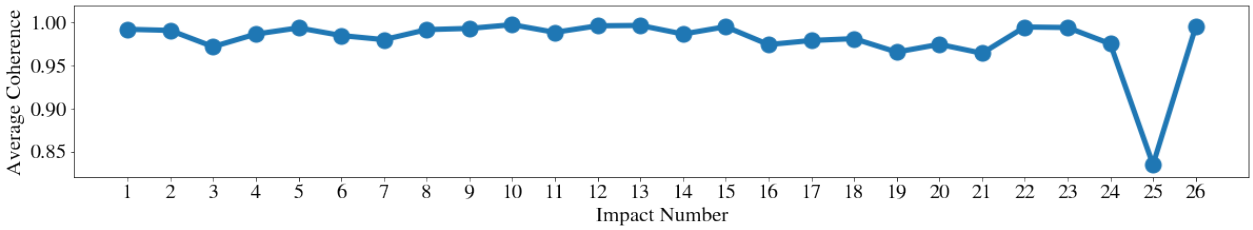

Figure 6: The average coherence given the original positions are calculated via equation (7) and (8). The coherence is calculated between the experimental response after a given impact and the reconstructed response in same position. The reconstructions are a result of Step 1 - 4 in Figure 3.

The proposed framework, Figure 3, can only update one problem at a time (e.g., a sensor position in x direction or all impact positions in y direction), as looping over all possibilities at once is too computationally cumbersome. Note that with no noise on the data, the framework works perfectly and completely recovers the true positions. With noise, we seek positions closer to the "true values," than originally defined, but it is expected that the framework is not entirely accurate. When defining measurement points, it is also worth noting that some positions are unfeasible to hit in practice. As an example, numerically, an FRF measured on the centerline after an impact enforced exactly on the centerline will not induce torsional modes. However, the torsion modes will be excited experimentally, as the impact and sensor measurement position/direction are imperfect. The same goes for the nodal points. If the impact is numerically defined at a nodal point of a mode, that mode will not be excited. Once again, perfection is only a numerical concept.

We now run the framework described in Figure 3 to find the optimal positions. We only consider the measured accelerometer response in z, as it aligns with the impact direction. First, we identify if the y position of the sensor is optimal. We find that the y-position agreeing the best over all the impacts is 140.5 mm (not illustrated here), thus a 0.5 mm shifted compared to original definition, which agrees with the shift we enforced. Then we test different y-positions of the impacts and find the optimal for all impacts. The y positions are tested first, as they plays the biggest role w.r.t. the amplitude of the y and z bending modes (which counts for 7 of the 10 modes in the frequency spectrum). Figure 7 shows the average coherence when testing different impact positions (± 2 mm), for all 26 impacts. Making these small corrections, the average coherence increases to 0.99 for all impacts. In many applications that would probably be sufficient, and not further corrections would be needed.

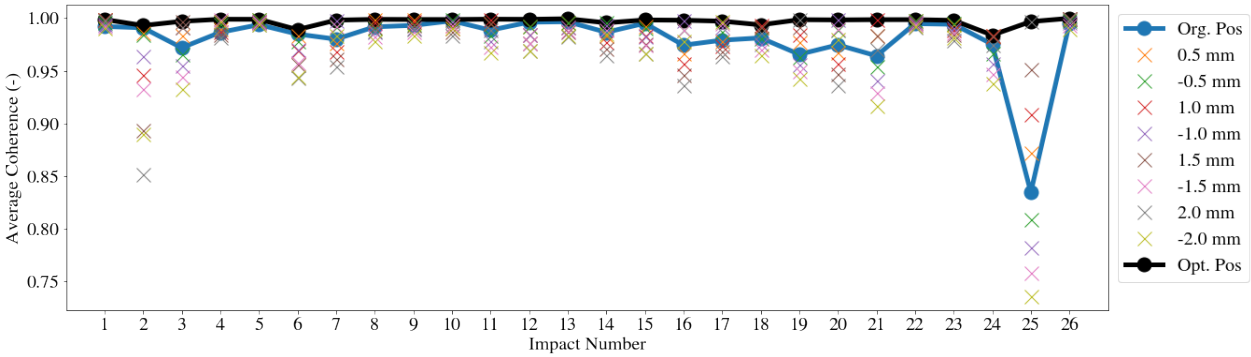

Figure 7: Average coherence for different y positions ($\pm$ 2 mm) of the impacts.

In this case, we however continue the correction. We have now remedied the y-positions, which influence the response the most, now we try to update the x-positions, to even further enhance the correlation. The framework reveals that the optimum sensor position is in 23.8 mm, thus a -1 mm shift from the original definition, which is correct. Running the framework for the x-positions of the impacts, we find (see Figure 8), that we can get a coherence very close to 1. And why is the coherence now not perfect? For one, the experimental data is noisy, which will cause a small discrepancy, and the updated positions are not perfect. In y-direction, the framework makes a 0.5 mm mistake at Impact 14 and a -0.5 mm mistake at Impact 24. In x-direction, the framework makes a -0.5 mm mistake at Impact 5, 0.5 mm at Impact 13, and -1 mm at Impact 14. This is acceptable, and the final result is definitely better than the original positions. Figure 9 shows the parent model data for Impact 25, after using the framework, and the improved agreement with the simulated experiment is very evident, especially around the antiresonance at 3400 Hz.

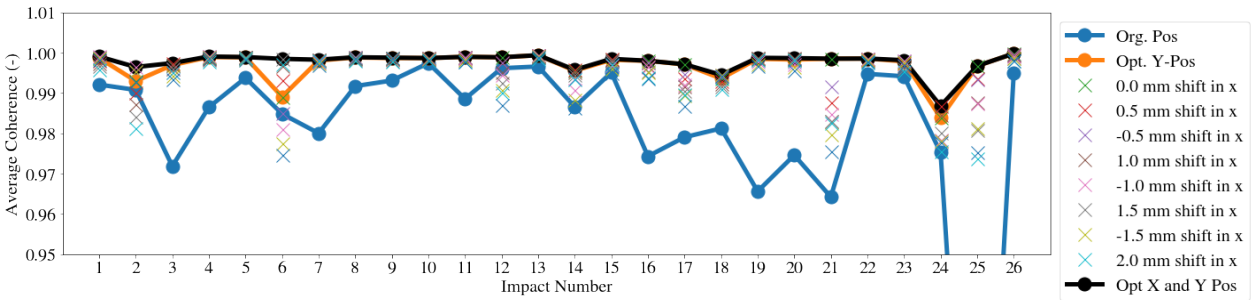

Figure 8: Optimizing the x position. To better show the fine differences, the coherence limits are [0.95-1.01]. For full view of the original position coherence (blue line) see Figure 6.

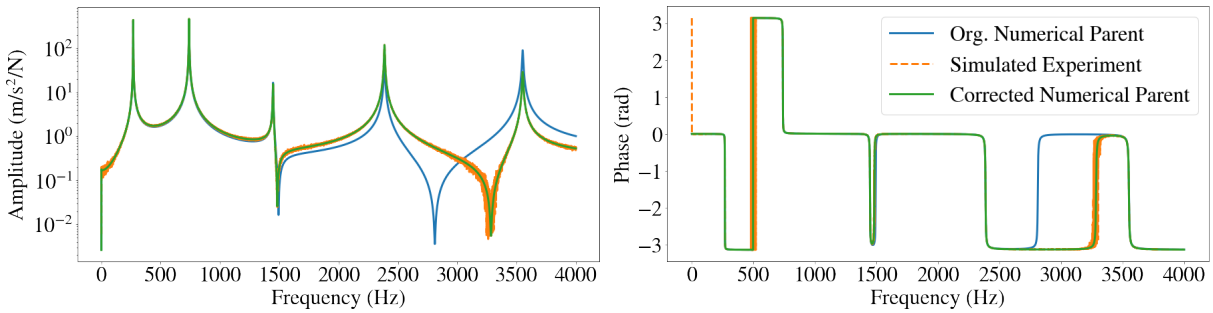

Figure 9: Example FRF of the original and corrected parent model and the simulated measured response. The z response of the accelerometer, after Impact 25 at the y-position 372.5 mm.

We have now demonstrated that the framework can recover the correct positions, with few and minor deviations, significantly improving the agreement between a parent model and experimental data. With improved correlation between a parent model and experimental data, a hybrid SEMM model will be much more accurate. In this numerical case, where the simulated experiment *is* the numerical model, just with noise, the hybrid SEMM model will not differ from the updated parent model. In the case of actual experimental data, there will always be a discrepancy between model FRFs and experimental FRFs. The discrepancy arises from many sources, particularly from inaccurately defined boundary, material and geometrical parameters. The following section will conclude by demonstrating what can be gained by making a position-corrected hybrid SEMM model based on actual experimental data.

5 Experimental test

We make a simple steel beam setup in the lab to test the novel framework's practical applicability. The dimensions of the beam are the same as the numerical beam used for the validation ($49.6 \times 400 \times 8.5$ mm^3). The experiment is identical to the numerical validation, with the only difference being that in the experimental case, we do not know the *actual* positions. The beam is placed on two foam pieces, and an accelerometer is attached with wax underneath it. We impact the hammer on the top, along the centerline. The experimental beam has the same material properties as that used in the numerical validation, and the numerical model is now our parent model. The impact hammer used for the experiment has a tip width of approximately 5 mm. Therefore, we deem it realistic that the hit position is up to ± 2 mm off target—the more trained a modal tester, the less variation to be expected.

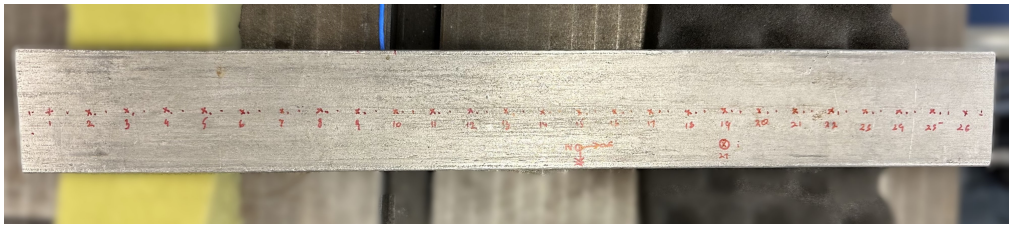

Figure 10: Beam on foam in lab.

5.1 Results

First, we apply the identification framework from [6] (Step 1-4 in Figure 3) using the originally defined positions from Table 2. That gives us the correlation diagram in Figure 11. The correlations are high for almost all points (not so surprising, as the setup is very simple). However, there are still a few outliers (Impact 2, 21 and 25, in particular). For more details, Figure 12 shows an example FRF of the response after Impact 2 (the one showing the lowest correlation). The experimental response captures modes not present in the numerical model at that DoF. It captures the first torsion mode at 1239 Hz, and the last two modes, mode 9 and mode 10, also appear in the experimental response. The experimental antiresonance around 3000 Hz is also not aligned with the parent model.

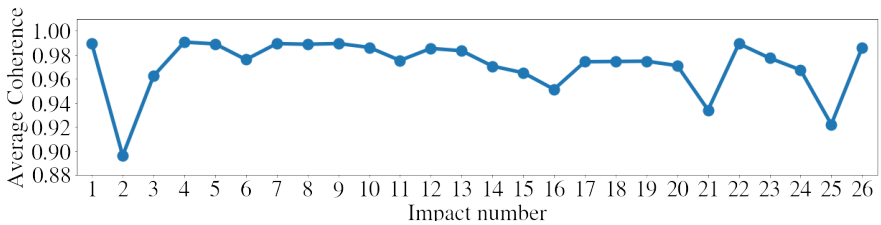

Figure 11: The average coherence for the original positions (result of Step 1-4).

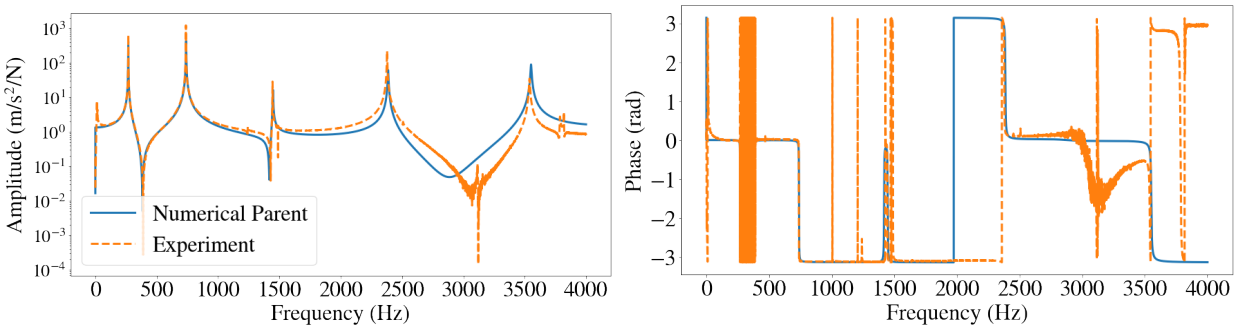

Figure 12: A FRF predicted by the parent model and the measured response at the same DoF. The measured z response of the accelerometer, after Impact 2, y position 27.5 mm, cf. Figure 4.

In [6], the next step would be to discard the worst measurements, e.g., 2, 21, and 25. We want to test if we can improve the correlations by slightly shifting the position of the hammer impacts, thus applying the complete framework of Figure 3. So far, the algorithm only works, taking one type of update at a time. We check if the sensor position in y is optimal and find that a shift of 1 mm gives a slight overall improvement (from an overall average of 0.971 to 0.976). We then test the impact positions in the y-direction. We loop over ± 2 mm in 0.5 mm steps and find we can improve the correlation to ≥ 0.96 for all impacts by slightly changing the positions. Figure 13 shows the result. Note that the coherence of Impact 2, 21, and 25 is especially improved, even though the corrections are only -1.5 mm, -2 mm, and -1.0 mm, respectively. When testing shifts in x positions of both the sensor and the impacts, we see no noteworthy improvement when updating the positions.

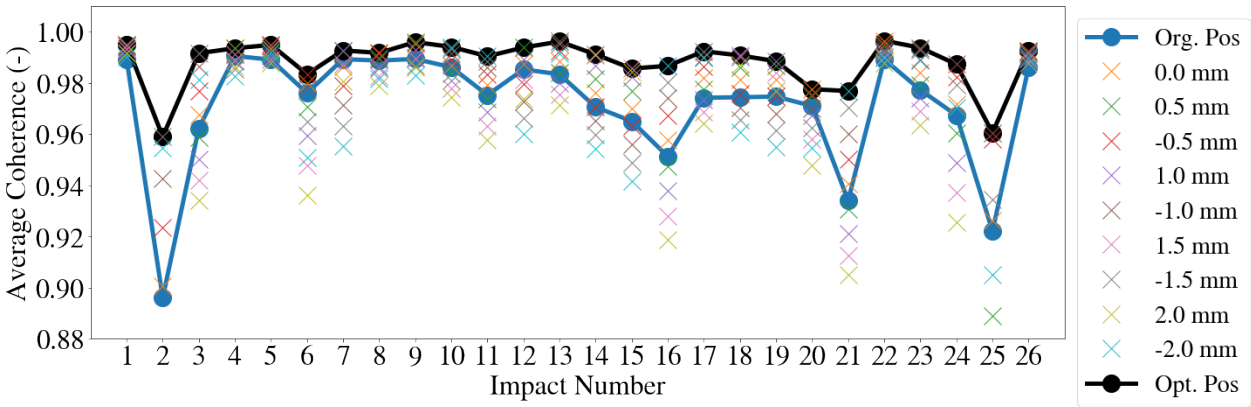

Figure 13: The average coherence are calculated via equation (7) and (8). The coherence is calculated between the experimental response after a given impact and the reconstructed response in same position. The reconstructions are a result of Step 1 - 4. The shifts are in the longitudinal direction (y direction).

Figure 14 shows the response after Impact 2 of the original and corrected parent model. The improvement is especially evident around the antiresonance at 3200 Hz. Assuming no correction was made, 15 of 26 responses had an average coherence under 0.98. By applying the framework, all but 4 impacts reach a coherence above 0.98, and the overall average increases from 0.971 to 0.988. A beam on foam is a very simple experiment, so the coherence values are high from the beginning. However, the coherence values become almost perfect just by shifting the positions ± 2 mm. How much one wants to correct can depend on the purpose. It takes some time to run the identification algorithm, and if the correlations are already close to 1, it may not be necessary. However, in cases where some of the measurement data fits quite poorly with a numerical model, there might be much to gain by ensuring the metadata is appropriately chosen.

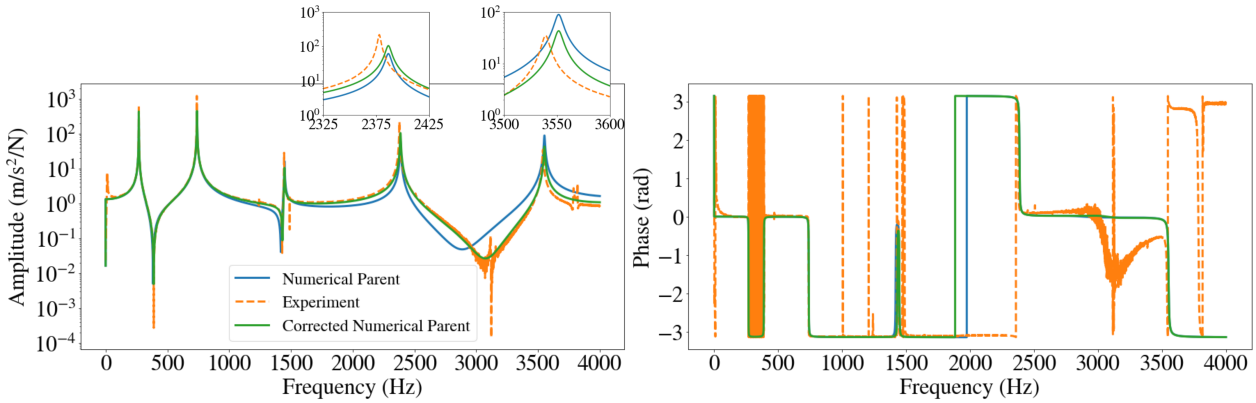

Figure 14: A frequency response function predicted by the parent model and the measured response at the same DoF. The measured z response of the accelerometer, after Impact 2.

At first glance at the full frequency range of Figure 14, it appears that further applying SEMM is unnecessary, as the corrected numerical model performs so well, giving predictions very similar to the experimental observations. However, when zooming in on the peaks, it is evident that the numerical model is slightly off. The peak shifts are due to the fact that the numerically defined material parameters and beam dimensions are not exactly the same as the experimental. Returning to the title of this paper, we want to improve hybrid modelling. By applying SEMM using the corrected numerical model, we can achieve a high fidelity hybrid model exhibiting extremely high agreement with experimental observations. Figure 15 shows the result for Impact 2. The SEMM procedure has an amazing ability to accurately capture the experimentally observed natural frequencies (a product of the enforced compatibility and force equilibrium). Note that SEMM captures the natural frequencies even if we do not improve the metadata of the parent model. However, with a corrected parent model, we can achieve an SEMM result that not only captures the natural frequencies but also follows the experimentally observed amplitude level over the whole frequency range (both the antiresonances and the modal damping levels are well captured).

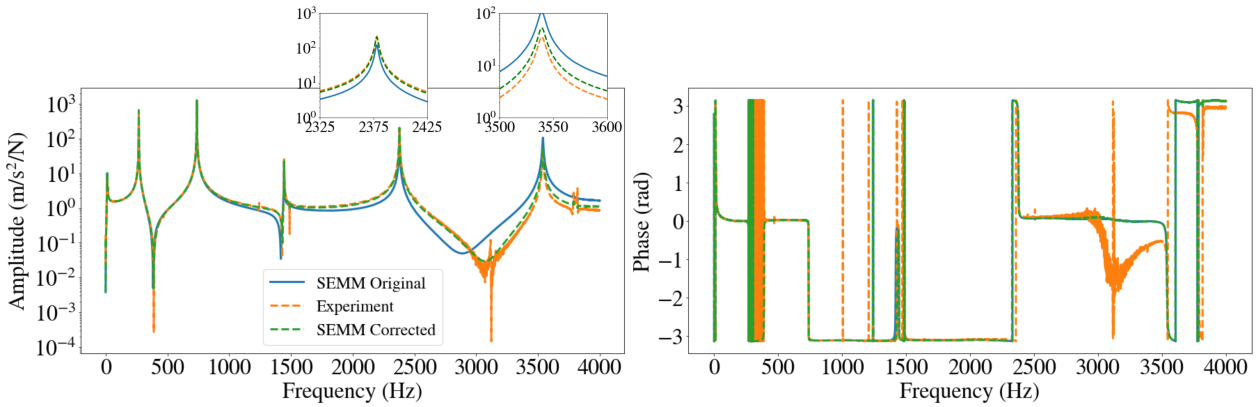

Figure 15: A frequency response function predicted by the SEMM model and the measured response at the same DoF. The measured z response of the accelerometer, after Impact 2.

6 Discussion

We have demonstrated, both numerically and experimentally that by using this novel framework, and thus slightly shifting the position of an impact, we can improve the correlation between experiment and numerical model significantly. The *true* position is unknown, but the assumption is that the better the correlation, the

more likely it is the correct position. In this work we only shift the positions, it is also possible to shift the direction of an impact. The principle is the same. The only thing to be aware of is that the directions and positions interact. It plays no role to have a tilted hit, if the sensor is on a nodal line (as was the case here). Relooking at Figure 14, it is evident that mode 9 and 10 appears in the experimental response, but still not in the corrected numerical parent. This discrepancy happens, as mode 9 and 10 numerically has zero amplitude at the position of Impact 2. A further development of the framework could be searching for an combined direction/position/impact/sensor optimum, not only one thing at a time. Also, using just the average coherence as a measure for the quality is a rather coarse approach. E.g., capturing mode 9 and 10 in the numerical parent for Impact 2, would probably not improve the average coherence very much. In such a case, the FRAC value might be a better measure, as it is very sensitive to the position of peaks.

A reasonable question is whether these slight refinements are important, as they naturally do not change the measured natural frequencies. However, we often want to use frequency-based substructuring to couple structures together, and then positioning errors propagate. Take the classical tool of the Virtual Point transformation [9, 10]. Here experimental data is transformed into a virtual position. However, if the defined position of the measurement data is wrong, the virtual point response will also be wrong.

7 Conclusions

In this work, we suggest a novel framework for updating the metadata of a modal analysis measurement campaign. Using the underlying information of a numerical model, we tune the experimental metadata to get the best correlation. Some DoFs responses are very susceptible to even the slightest shift in position. Changing the position as little as a single millimeter can vastly change the response, especially around antiresonances. The antiresonances are usually not that important for dynamicists, but the response obtained when coupling two structures where the antiresonances are slightly off will be strongly affected. The experimental beam test of the framework improved the average coherence from 0.971 to 0.988. Every single response was improved by applying shifts of only ± 2 mm. Even the worst outlier, with an average coherence below 0.90, was improved to 0.96 by shifting the position 1.5 mm to one side. Finally, when applying SEMM using the experimental data and the corrected numerical model, a very accurate high-fidelity hybrid model was obtained, capturing not only the natural frequencies but also the experimentally observed amplitude level over the whole frequency range.

Acknowledgements

This work was supported by a research grant (41392) from VILLUM FONDEN.

References

[1] D. de Klerk, D. J. Rixen, and S. N. Voormeeren, "General Framework for Dynamic Substructuring: History, Review and Classification of Techniques," *AIAA Journal*, vol. 46, no. 5, pp. 1169–1181, may 2008. [Online]. Available: https://doi.org/10.2514/1.33274

[2] M. S. Allen, D. Rixen, M. n van der Seijs, T. Paolo, Abrahamsson;Thomas, and R. L. Mayes, *Substructuring in Engineering Dynamics*. Springer International Publishing, 2020.

[3] D. Nicgorski and P. Avitabile, "Experimental issues related to frequency response function measurements for frequency-based substructuring," *Mechanical Systems and Signal Processing*, vol. 24, no. 5, pp. 1324–1337, 2010, special Issue: Operational Modal Analysis. [Online]. Available: https://www.sciencedirect.com/science/article/pii/S0888327009002660

[4] J. W. R. Meggitt, "On the treatment of uncertainty in experimentally measured frequency response functions," *Metrologia*, vol. 55, no. 6, p. 806, oct 2018. [Online]. Available: https://dx.doi.org/10.1088/1681-7575/aadeeb

[5] M. Brøns and D. J. Rixen, "Dynamic disturbance substructuring: identifying localized nonlinear vibrations," in *Proceedings of ISMA2022 International Conference on Noise and Vibration Engineering and USD2022 International Conference on Uncertainty in Structural Dynamics*, 2022.

[6] M. Kodrič, G. Čepon, and M. Boltežar, "Experimental framework for identifying inconsistent measurements in frequency-based substructuring," *Mechanical Systems and Signal Processing*, vol. 154, 2021.

[7] S. W. Klaassen, M. V. van der Seijs, and D. de Klerk, "System equivalent model mixing," *Mechanical Systems and Signal Processing*, vol. 105, pp. 90–112, 2018. [Online]. Available: https://doi.org/10.1016/j.ymssp.2017.12.003

[8] T. Bregar, A. E. Mahmoudi, M. Kodrič, D. Ocepek, F. Trainotti, M. Pogačar, M. Göldeli, G. Čepon, M. Boltežar, and D. J. Rixen, "pyfbs: A python package for frequency based substructuring," *Journal of Open Source Software*, vol. 7, no. 69, p. 3399, 2022. [Online]. Available: https://doi.org/10.21105/joss.03399

[9] M. Haeussler, S. W. Klaassen, and D. J. Rixen, "Experimental twelve degree of freedom rubber isolator models for use in substructuring assemblies," *Journal of Sound and Vibration*, vol. 474, pp. 9–11, 2020.

[10] T. Bregar, N. Holeček, G. Čepon, D. J. Rixen, and M. Boltežar, "Including directly measured rotations in the virtual point transformation," *Mechanical Systems and Signal Processing*, vol. 141, p. 106440, 2020.